

## Source localization in the ocean by replica subspace intersection method

S. LAKSHMIPATHI AND G. V. ANAND

Department of Electrical Communication Engineering, Indian Institute of Science, Bangalore 560 012, India  
e-mails: slpathi@protocol.ece.iisc.ernet.in, anandgv@ece.iisc.ernet.in

### Abstract

Source localization by matched field processing (MFP) involves accurate modeling of the ocean and projection of the replica pressure vectors for hypothetical source positions on to the array data vector or the noise subspace obtained by eigendecomposition of the array data correlation matrix. The performance of all matched field processors is degraded by the noncoincidence of the source coordinates with one of the grid coordinates of the search grid. A new method of range–depth localization, called the replica subspace intersection (RESIN) method, is presented in this paper. The RESIN method exploits the relationship between the replica subspaces and the signal subspace. It is shown that the RESIN processor is more tolerant to mismatch between source coordinates and the nearest grid coordinates than other commonly used processors such as Bartlett and MUSIC. This gridding mismatch tolerance can be exploited to increase search grid spacing and thus reduce the computational complexity of the search.

**Keywords:** Matched field processing, replica subspace, subspace intersection, gridding mismatch.

### 1. Introduction

Matched field processing (MFP) techniques of source localization in the ocean have been studied extensively both theoretically and experimentally.<sup>1</sup> The source coordinates are estimated from the positions of the peaks of an ambiguity function that is constructed by projecting the replica vectors computed for different hypothetical source positions either on to the array data vector or on to the noise subspace obtained by eigendecomposition of the array data covariance matrix. The performance of MFP depends on the accuracy with which the environmental parameters are known. Satisfactory performance also requires the use of a sufficiently fine search grid to ensure that one of the search points is sufficiently close to the actual position of each source. The Bartlett processor has a greater tolerance to mismatch than most other processors, but the former cannot be used for multiple source localization. Subspace-based methods such as MUSIC<sup>2, 3</sup> are capable of localizing multiple sources with high resolution, but they are very sensitive to mismatch. In this paper, we propose a new method of range–depth localization of multiple sources, based on the concept of replica subspace of Harrison.<sup>4</sup> Harrison projects the data vector on a weighted replica subspace and obtains estimates of all unknown parameters by the maximum likelihood method. Our method exploits the relationship between the replica subspaces and the signal subspace derived by eigendecomposition of the array data correlation matrix. It is shown that the new method, called the replica subspace intersection (RESIN) method, can tolerate a larger mismatch between the source coordinates and the nearest search-grid coordinates than

either MUSIC or the Bartlett method. Greater tolerance to gridding mismatch permits the use of a coarser gridding which can lead to a significant reduction in computational complexity.

In Section 2, the signal subspace of a linear vertical array is derived. The RESIN method of range–depth localization is presented in Section 3. In Section 4, simulation results are presented for single- and multisource scenarios to demonstrate the robustness of the RESIN technique to gridding mismatch.

## 2. Eigendecomposition of the correlation matrix

The ocean is modelled as a horizontally stratified water layer of constant depth  $d$  overlying a horizontally stratified bottom. Let  $J$  mutually uncorrelated narrowband sources of center frequency  $f_0$  be located at depths  $z_j$ ,  $j = 1, \dots, J$  with respect to a vertical linear array of  $N$  hydrophones. Let the hydrophone depths be denoted by  $z'_n$ ,  $n = 1, \dots, N$ . The signal at the  $n$ th hydrophone due to the  $j$ th source is given by

$$s_{jn}(t) = p_{jn} b_j(t) e^{-i2\pi f_0 t}, \quad j = 1, \dots, J; \quad n = 1, \dots, N \quad (1)$$

where  $b_j(t)$  is a slowly varying zero-mean random function that accounts for the random fluctuations of the source and the intervening medium, and the variance of  $b_j(t)$  given by

$$\sigma_j^2 = E[b_j^2(t)] \quad (2)$$

is a measure of the strength of the source. Under far-field conditions, the signal amplitudes  $p_{jn}$  can be written in terms of the discrete normal modes of the channel<sup>5</sup>

$$p_{jn} = \sum_{m=1}^M x_{jm} \psi_m(z'_n), \quad j = 1, \dots, J; \quad n = 1, \dots, N \quad (3)$$

$$x_{jm} = \left( \frac{2\pi}{k_m r_j} \right)^{1/2} \psi_m(z_j) \psi_m(z'_n) e^{-\alpha_m r_j + i(k_m r_j + \pi/4)}, \quad (4)$$

where the mode functions (eigenfunctions)  $\psi_m(z)$ , the modal wavenumbers  $k_m$ , and the attenuation constants  $\alpha_m$  are all dependent on the frequency  $f_0$ . The array signal amplitude vector due to the  $j$ th source can be written as

$$\begin{aligned} \mathbf{p}(r_j, z_j) &= [p_{j1} \dots p_{jN}]^T \\ &= \Psi [x_{j1} \dots x_{jM}]^T, \end{aligned} \quad (5)$$

where

$$\Psi = \begin{bmatrix} \psi_1(z'_1) & \dots & \psi_M(z'_1) \\ \vdots & \vdots & \vdots \\ \psi_1(z'_N) & \dots & \psi_M(z'_N) \end{bmatrix}. \quad (6)$$

The array signal-plus-noise vector  $\mathbf{y}(t) = [y_1(t) \dots y_N(t)]^T$  is given by

$$\mathbf{y}(t) = \mathbf{P}\mathbf{b}(t)e^{-i2\pi f_0 t} + \mathbf{n}(t), \quad (7)$$

where  $\mathbf{n}(t)$  is the array noise vector, and

$$\mathbf{b}(t) = [b_1(t) \cdots b_J(t)]^T, \quad (8)$$

$$\begin{aligned} \mathbf{P} &= [\mathbf{p}(r_1, z_1) \cdots \mathbf{p}(r_J, z_J)] \\ &= \Psi\mathbf{X}, \end{aligned} \quad (9)$$

$$\mathbf{X} = \begin{bmatrix} x_{11} & \cdots & x_{J1} \\ \vdots & \vdots & \vdots \\ x_{1M} & \cdots & x_{JM} \end{bmatrix} \quad (10)$$

Assuming that  $N \geq M \geq J$ , the matrix  $\Psi$  has rank  $M$ , and the matrices  $\mathbf{X}$  and  $\mathbf{P}$  have rank  $J$ .

Assuming that all the signals and noise are mutually uncorrelated and that the noise is spatially white, the array spectral correlation matrix at frequency  $f_0$  can be written as

$$\begin{aligned} \mathbf{R} &= E[\hat{\mathbf{y}}(f_0)\hat{\mathbf{y}}^H(f_0)] \\ &= \mathbf{P}\mathbf{S}\mathbf{P}^H + \sigma^2\mathbf{I}, \end{aligned} \quad (11)$$

where  $\hat{\mathbf{y}}(f_0)$  denotes the discrete Fourier transform at frequency  $f_0$  of a filtered and sampled version of  $\mathbf{y}(t)$ ,

$$\mathbf{S} = \text{diag}(\sigma_1^2, \dots, \sigma_J^2), \quad (12)$$

$\sigma^2$  the noise variance, and  $\mathbf{I}$  the identity matrix. The eigendecomposition of  $\mathbf{R}$  is given by

$$\mathbf{R} = \sum_{i=1}^N \lambda_i \mathbf{u}_i \mathbf{u}_i^H. \quad (13)$$

The eigenvalues may be ordered as  $\lambda_1 \geq \lambda_2 \geq \dots \geq \lambda_J > \lambda_{J+1} = \dots = \lambda_N$ , where

$$\lambda_i = \begin{cases} v_i + \sigma^2 & \text{for } i = 1, \dots, J \\ \sigma^2 & \text{for } i = J+1, \dots, N, \end{cases} \quad (14)$$

and  $v_1, \dots, v_J$  are the eigenvalues of the rank- $J$  matrix  $\mathbf{P}\mathbf{S}\mathbf{P}^H$ . The eigenvalues  $\lambda_1, \dots, \lambda_J$  are called signal eigenvalues and the corresponding eigenvectors  $\mathbf{u}_1, \dots, \mathbf{u}_J$  form an orthonormal basis of the signal subspace  $\mathcal{S}$  defined as

$$\begin{aligned} \mathcal{S} &= \text{span}\{\mathbf{p}(r_1, z_1), \dots, \mathbf{p}(r_J, z_J)\} \\ &= \text{span}\{\mathbf{u}_1, \dots, \mathbf{u}_J\}. \end{aligned} \quad (15)$$

### 3. Replica subspace intersection method

In all matched field processors, the array spectral data vector  $\hat{\mathbf{y}}(f_0)$  is compared with a series of replica vectors  $\boldsymbol{\theta}(r, z)$ , defined as the normalized signal amplitude vectors

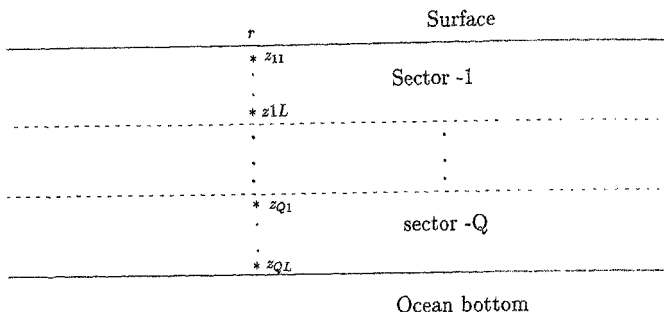


FIG. 1. Partitioning of the ocean depth  $d$  into  $Q$  equal sectors.  $z_{ql}$ ,  $l = 1, \dots, L$ ;  $q = 1, \dots, Q$  represent the  $l$  test depths in the  $q$ th sector.

$$\mathbf{e}(r, z) = \frac{\mathbf{p}(r, z)}{|\mathbf{p}(r, z)|}, \quad (16)$$

for different test positions  $(r, z)$  in the search region. It may be noted that  $\mathbf{e}(r, z)$  depend on  $f_0$ . In the present method, instead of processing each replica vector separately, we process blocks of  $L$  replica vectors. For this purpose, we partition the total ocean depth  $d$  into  $Q$  equal sectors and choose  $L$  test depths  $z_{q1}, \dots, z_{qL}$  at uniform intervals within each sector (Fig. 1), so that

$$\begin{aligned} z_{qi} &= [(q-1)L + i - 1/2]\Delta z, \\ q &= 1, \dots, Q; i = 1, \dots, L; \\ \Delta z &= d/QL. \end{aligned} \quad (17)$$

Thus, for each test range  $r$  and depth sector  $q$ , we have a block of  $L$  replica vectors  $\mathbf{e}(r, z_{qi})$ ,  $i = 1, \dots, L$ , which are linearly independent if  $L \leq M$ . Let the replica subspace  $\mathfrak{v}_q(r)$  be defined as

$$\mathfrak{v}_q(r) = \text{span}\{\mathbf{e}(r, z_{q1}), \dots, \mathbf{e}(r, z_{qL})\}. \quad (18)$$

If  $L \leq M - J$ , the replica subspace  $\mathfrak{v}_q(r)$  and the signal subspace  $\mathcal{S} = \text{span}\{\mathbf{p}(r_1, z_1), \dots, \mathbf{p}(r_J, z_J)\}$  intersect if and only if one of the test coordinates  $(r, z_{qi})$ ,  $i = 1, \dots, L$  coincides with one of the source coordinates  $(r_j, z_j)$ ,  $j = 1, \dots, J$ . This subspace intersection property can be exploited to estimate the range and the depth sector of each source.

A simple procedure to test whether  $\mathfrak{v}_q(r)$  and  $\mathcal{S}$  intersect or not is described below. Consider the matrix  $\mathbf{D}_q(r)$  with  $N$  rows and  $P = L + J$  columns, obtained by stacking together all the spanning vectors of  $\mathfrak{v}_q(r)$  and the orthonormal basis vectors  $\mathbf{u}_1, \dots, \mathbf{u}_J$  of  $\mathcal{S}$ , i.e.

$$\mathbf{D}_q(r) = [\mathbf{e}(r, z_{q1}) \cdots \mathbf{e}(r, z_{qL}) \mathbf{u}_1 \cdots \mathbf{u}_J]. \quad (19)$$

The QR decomposition of  $D_q(r)$  yields<sup>6</sup>

$$D_q(r) = Q_q(r)R_q(r), \quad (20)$$

where  $Q_q(r)$  is an  $N \times P$  matrix with orthonormal columns and  $R_q(r)$  is a  $P \times P$  upper triangular matrix. If  $v_q(r)$  and  $\mathcal{S}$  are non-intersecting subspaces, all the diagonal elements of  $R_q(r)$  are non-zero. But if these subspaces intersect, at least one of the last  $J$  diagonal elements of  $R_q(r)$  is equal to zero. Let  $R_{q,jl}(r)$  denote the  $j$ th diagonal element of  $R_q(r)$ , and define

$$B_{\text{RESIN}}(r) = \left[ \min_{1 \leq q \leq Q} \min_{L+1 \leq j \leq P} R_{q,jl}(r) \right]^{-1}. \quad (21)$$

The  $J$  highest peaks of  $B_{\text{RESIN}}(r)$  provide range estimates  $\hat{r}_j$  and depth sector estimates  $\hat{g}_j$  of the sources. A better estimate of each source depth can be obtained by carrying out an 1-dimensional search within the identified depth sector at the estimated range  $\hat{r}_j$ .

#### 4. Simulation results

Computer simulation results are presented for a shallow Pekeris channel with the following parameters: channel depth  $d = 100$  m, sound speed in water  $c_w = 1500$  m/s, sound speed at

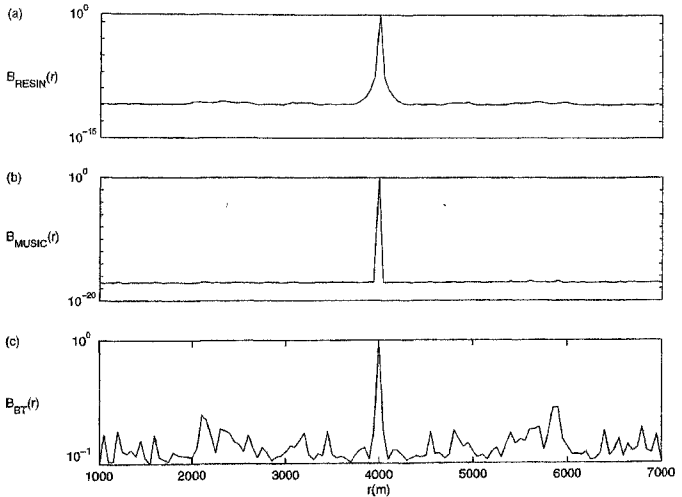


FIG. 2. Range ambiguity functions of the RESIN, MUSIC and Bartlett processors for a source at 4000 m range and 31 m depth. Source position coincides with a grid point.

the bottom  $c_b = 1700$  m/s, bottom-to-water density ratio  $\rho = 1.5$ , bottom attenuation  $\alpha = 0.5$  dB/wavelength, source frequency  $f_0 = 200$  Hz. The number of discrete modes in the channel at this frequency is  $M = 12$ . A uniform linear array of  $N = 20$  hydrophones with 5-m spacing spans the channel, the depth of the  $n$ th hydrophone being  $z_n = 5(n - 1) + 1$ .

In all the simulations, the search grid has 5-m spacing in depth. In range, the spacing is allowed to vary from 25 to 100 m. In RESIN simulations, the water column is divided into two depth sectors; the grid points lie at depths of 1, 6, ..., 46 m in the first sector and at 51, 56, ..., 96 m in the second sector. The RESIN range ambiguity function is given by eqn (21). The range ambiguity functions of the Bartlett<sup>1</sup> and MUSIC<sup>3</sup> processors, given by

$$B_{BT}(r) = \max_z e^{H}(r, z) \mathbf{R} e(r, z), \quad (22)$$

and

$$B_{MUSIC}(r) = \max_z \left[ \sum_{n=j-1}^N e^{H}(r, z) u_n u_n^H e(r, z) \right]^{-1} \quad (23)$$

are also plotted for comparison.

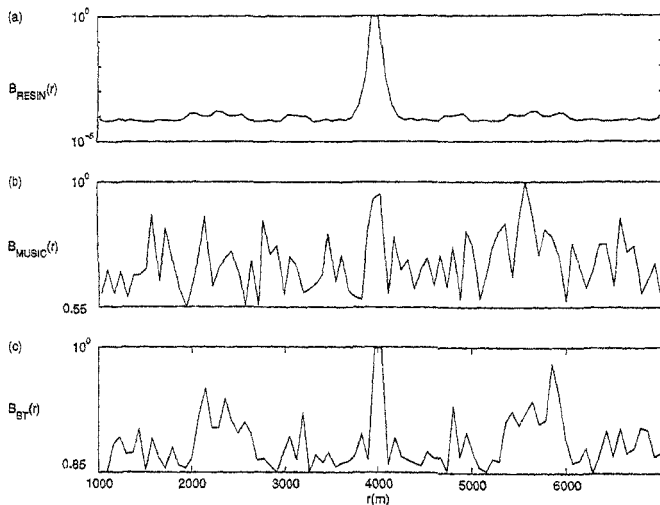


FIG. 3. Range ambiguity functions for sources at (4000 m, 33.5 m). Source is away from the nearest grid point by 35 m in range and 2.5 m in depth.

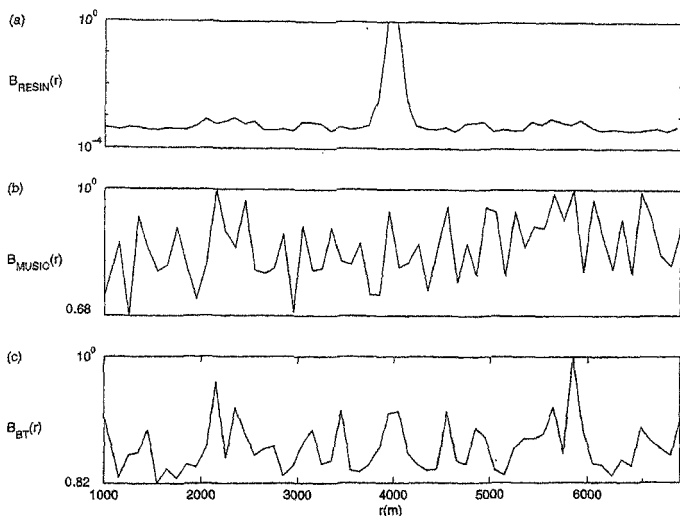


FIG. 4. Range ambiguity functions for a source at (4000 m, 33.5 m) when the source is away from the nearest grid point by 50 m in range and 2.5 m in depth.

The results shown in Figs 2–5 assume 10 dB SNR and a perfect knowledge of the correlation matrix  $R$  (asymptotic or infinite-data case). Figure 2 shows the range localization of a source at 4000 m range and 31 m depth by RESIN, MUSIC and Bartlett techniques. The search grid has a 25-m spacing in range, and one of the grid points coincides with the source position. The MUSIC ambiguity function has a very high peak (about 170 dB above the background) with a very narrow base. The peak of the RESIN ambiguity function, at 110 dB above the background, is lower than that of MUSIC but much higher than that of Bartlett which rises less than 10 dB above the background. But the base of the RESIN peak is much wider than that of the others. It is this combination of a high peak with a wide base that gives the RESIN processor a high degree of tolerance to gridding mismatch. In Figs 3 and 4 the source is at (4000 m, 33.5 m). In Fig. 3, the range-spacing of the search grid is 70 m, and the source is away from the nearest grid point by 35 m in range and 2.5 m in depth. The MUSIC processor is unable to localize the source. The Bartlett processor is able to localize, but some of the sidelobes are very high. The peak of the RESIN processor stands out very clearly. In Fig. 4, the range spacing of the search grid is 100 m, and the source is away from the nearest grid point by 50 m in range and 2.5 m in depth. Both the MUSIC and the Bartlett processors fail to localize the source. The RESIN processor can still localize the source, though the peak is lower and blunter than that in Fig. 3. Figures 5 and 6 illustrate the multisource localization

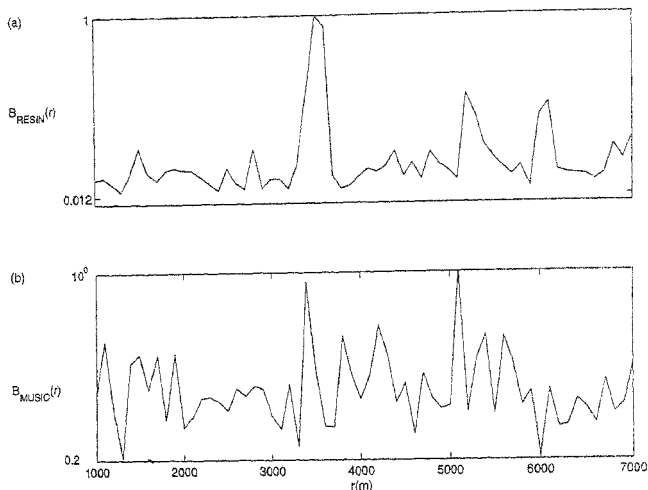


Fig. 5. Range ambiguity functions for three sources at (3550 m, 73.5 m), (5250 m, 33.5 m) and (6050 m, 23.5 m). All sources are away from the nearest grid point by 50 m in range and 2.5 m in depth.

capability of the RESIN processor. Bartlett ambiguity function is not included in these figures since this processor cannot localize multiple sources. Three sources are present at (6050 m, 23.5 m), (3550 m, 73.5 m) and (5250 m, 33.5 m). The range spacing of the search grid is 100 m, and the sources are away from the nearest grid points by 50 m in range and 2.5 m in depth. Figure 5 corresponds to the asymptotic case with 10 dB SNR and Fig. 6 to the finite-data case with 30 dB SNR. In the finite data case, the correlation matrix  $R$  is estimated from 200 snapshots of the data vector. The plots in Fig. 5 are obtained by averaging 25 Monte Carlo simulations. In Figs 5 and 6, the MUSIC processor is able to localize only two sources whereas the RESIN processor localizes all the three.

## 5. Conclusions

A replica subspace intersection (RESIN) method of source localization is presented in this paper. In MFP, a source may not be localized if the search grid is not fine enough to ensure that one of the grid points lies sufficiently close to the source. In the RESIN technique, replica vectors are processed in blocks by forming replica subspaces and projecting them on to the signal subspace. This procedure imparts greater tolerance to coarse range gridding as compared to the existing MFP processors.

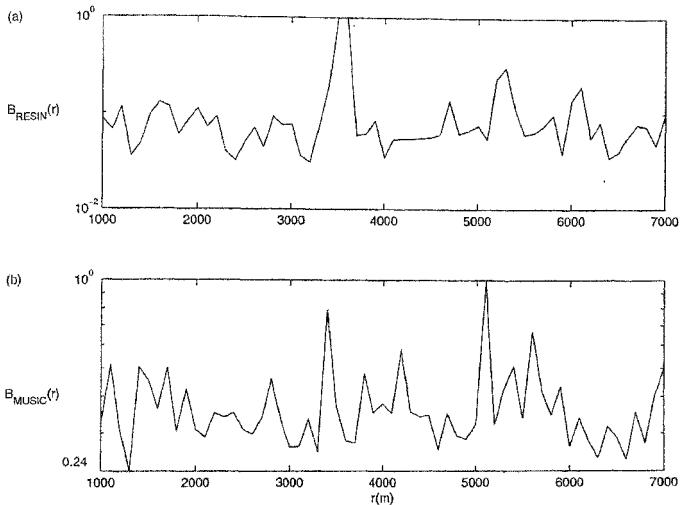


FIG. 6. Range ambiguity functions for the finite data case.  $R$  is estimated from 200 snapshots. Other conditions are the same as in Fig. 5.

### Acknowledgment

This work was supported by the Naval Physical and Oceanographic Laboratory, Kochi, India.

### References

1. TOLSTOY, A. *Matched field processing for underwater acoustics*, World Scientific, 1993.
2. OZARD, J. M. Matched field processing in shallow water for range, depth and bearing determination: Results of experiment and simulation, *J. Acoust. Soc. Am.*, 1989, **86**, 744-753.
3. SCHMIDT, R. O. Multiple emitter location and signal parameter estimation, *Proc. RADC Spectrum Estimation Workshop*, Rome Air Development Center, Rome, 1979, pp. 243-258.
4. HARRISON, B. F. *Robust matched-field processing: A subspace approach*, Ph.D. Thesis, Department of Electrical Engineering, University of Rhode Island, 1996.
5. BREKHOVSKIKH, L. M. AND LYSANOV, YU. *Fundamentals of ocean acoustics*, Ch. 5, Springer-Verlag, 1991.
6. GOLUB, G. H. AND VAN LOAN, C. F. *Matrix computations*, North Oxford Academic, London, 1996.